

Vertical Dry Adhesive Climbing with a 100x Bodyweight Payload

Elliot W. Hawkes^{1,2}, David L. Christensen^{1,2}, and Mark R. Cutkosky¹

Abstract—The ability to carry large payloads could greatly increase the applications of small, low cost climbing robots. We present a linear inchworm gait that uses a single powerful actuator to climb. To make this gait possible, we leveraged two new methods of achieving controllable, anisotropic adhesion (one method produces over 200 times stronger adhesion in the preferred direction). With controllable, anisotropic adhesion, the gait is robust to missed steps. In addition, the gait provides a stance in which the robot can rest without requiring power. An autonomous 9 gram robot is able to climb a smooth vertical surface at 3 mm/s, while hoisting more than a kilogram. We also present a scaled down version of the robot, which is considerably smaller than any previous dry adhesive climbing mechanism. It is actuated by externally powered Shape Memory Alloy, weighs 20 mg, and is capable of hoisting 500 mg. These climbers show that a large hoisting ability while climbing can be achieved using dry adhesives, and the presented concepts could aid in the development of autonomous, highly functional, small robots.

I. INTRODUCTION

Many insects are capable of exerting forces equivalent to many times their bodyweight. For instance, the Asian Weaver Ant (*Oecophylla smaragdina*) is capable of sustaining adhesion forces of over 100 times its own bodyweight [1], and with these forces has been documented to transport large vertebrate prey [2]. There are two crucial characteristics of insects that are capable of applying large forces, yet still easily locomote. First, they have incredible strength for their weight, or force density. Second, they have controllable adhesion, that can support large loads, yet can release easily from the surface when desired [3]. Without *controllable* adhesion, which can be switched on and off, small climbers would not be able to both apply large forces to objects and lift their feet to climb without exerting the same large forces at each step.

Previous adhesive climbing robots, while exhibiting impressive climbing, and in some cases maneuverability, have not come close to meeting the hoisting ability (defined here as payload normalized by bodyweight) of the weaver ant. Stickybot I could lift no more than 1 times its bodyweight, or roughly 300 g, [4], and Stickybot III a similar percentage, or 600 g [5]. Waalbot II could climb with 1.17 times its bodyweight, or 100 g [6]. In the realm of miniature adhesive climbing robots, defined here as less than 40 mm per side, only one example exists, which climbed with smooth rubber tank-treads [7]. It is the smallest vertical surface dry adhesive climber to date (10 g). The robot was built to carry no more

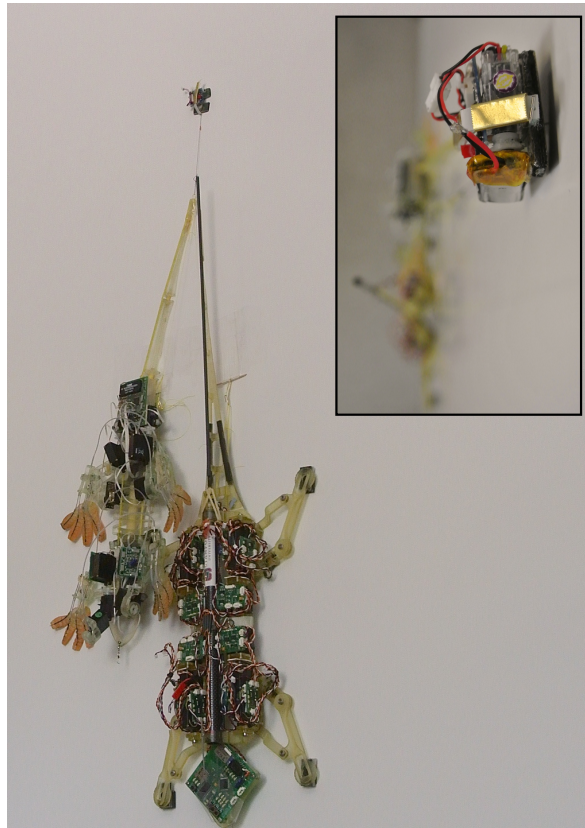


Fig. 1: The presented miniature 9 g climber hoisting Stickybot I and Stickybot III. *Inset*, View from the ceiling, looking down at the robots.

than 3 times its weight, or 30 g, and was tested up to a single bodyweight.

A small robot with the ability to hoist large loads could have countless applications not only in the oft-cited role as a small, cheap, disposable, mobile sensor in the realms of search and rescue, surveillance, and environmental monitoring, but also as an actor that could alter its environment. Instead of *observing* an event, a tiny robot that can produce huge forces could *affect* the event. It could (possibly in a team) carry a rope ladder to person trapped on the fifth floor of a burning building, or carry equipment and fix the crack it discovers in a dam or bridge.

While we are still far from realizing this vision, we have taken a step toward it with the creation of two novel methods of attaining controllable, anisotropic adhesion which enable a simple, 1 degree of freedom inchworm climbing gait. One method for anisotropy is based on applying moments to the adhesive pad to decrease contact area and thus adhesion, and

¹E.W. Hawkes, D.L. Christensen, and M.R. Cutkosky are with the Department of Mechanical Engineering at Stanford University, 450 Serra Mall, Stanford, CA 94305, U.S.A. ewhawkes at stanford.edu
² These authors contributed equally to the work.

the other uses sipping of the adhesive material to yield the same result. The gait displays robustness to missed steps; a climber does not fall, but rather remains in place and attempts another step. It also allows a climber to support the entire payload without power when adhered with its lower pad. We demonstrate the gait on two climbers. The first is a 9 g robot with onboard power and control, which uses a single servo to climb while hoisting a kilogram up a smooth vertical surface (Fig. 1). The second shows further miniaturization; it is an externally powered 20 mg climber that uses Shape Memory Alloy (SMA) as its actuator.

In this paper, we first present the design principles followed to create these two small climbers. Next, we describe the design specifications and fabrication. The results of tests are presented, as well as conclusions and future work.

II. DESIGN PRINCIPLES

Working at a small scale allows robots to be cheap and easily replaceable. Further, climbing with loads large relative to robot mass is easier at a small scale for two reasons. First, the square-cube law dictates that with isometric scaling, the mass of an object goes as the cube of the length scale, while the adhesive area goes as the square, and second, adhesive ability tends to drop off at larger scales, as exemplified by data from the gecko [8,9]. To carry large absolute loads, it is therefore desirable to make many small robots, each with a high relative hoisting ability, that work together to move the large load.

To create a small, simple robot with a large hoisting ability, a linear inchworm gait is chosen. This gait is based on the traditional inchworm motion, seen in numerous robots [10]–[13], including miniature [14,15] and even smaller [16]. One robot has shown climbing with penetrating spines on soft surfaces, lifting its bodyweight [17]. The novelty of the gait presented here, however, is that it allows a robot to climb up a smooth vertical surface using controllable dry adhesives, while supporting large loads, resisting falls due to missed steps, and parking without power consumption.

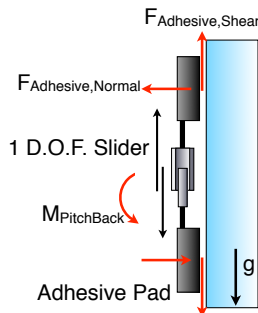


Fig. 2: A single degree of freedom, linear inchworm climbing gait.

The gait involves two adhesive pads that are able to move with respect to one another (Fig. 2). While one pad supports the load, the other moves up the wall. While this inchworm gait is conceptually very simple, the subtleties of achieving

the gait on a vertical surface while providing very large adhesive forces are more complex.

A. Uniform Loading

The first challenge is loading the adhesive uniformly to achieve the maximum possible adhesion. This is done through the use of a rigid adhesive pad and a tendon that loads the pad through its center of pressure. The payload is supported by this tendon, which avoids the moment that tends to pitch climbing robots backward (Fig. 2). The concept is described in [5].

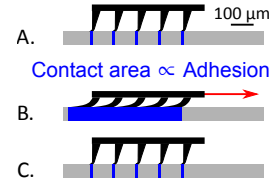


Fig. 3: A) Only the tips of the wedges engage with the surface at initial contact. B) When loaded in shear, the contact area, and thus the adhesion greatly increases. C) When unloaded, the contact area decreases as the wedges return to their neutral state, and the adhesion decreases to nearly zero.

B. Controllability

The second problem is sticking and unsticking the adhesive. Most adhesives, including many dry adhesives, require pressure in the normal direction to stick. With only a single degree of freedom, a linkage is required to press one adhesive pad into the surface while removing the other, all while progressing the robot up the wall. To avoid the use of a linkage, which adds weight to the robot, a *controllable* adhesive (capable of being turned on and off with the application of shear force), is used. The adhesive is Poly(dimethylsiloxane), or PDMS, microwedges [18]. When loaded in shear (along the surface) the adhesives pull themselves into contact, resulting in large adhesion (Fig. 3), but when unloaded, the adhesive can be easily removed from the surface. Controllability means that the robot only needs to transfer its weight to the adhesive to make it stick, without having to press it into the surface.

C. Anisotropy

The third challenge is moving the non-engaged adhesive pad up the wall during the “swing” phase of the gait. While controllability allows the easy engagement and release of the adhesive, it does not mean that the adhesive does not stick when sheared in the anti-preferred direction. In fact, a limit curve of the microwedges shows nearly symmetric performance in force space (Fig. 4). This is because the wedges simply flip, and the back of the wedge adheres.

The anisotropy ratio, α can be defined as

$$\alpha = \frac{A_{np}}{A_p} \quad (1)$$

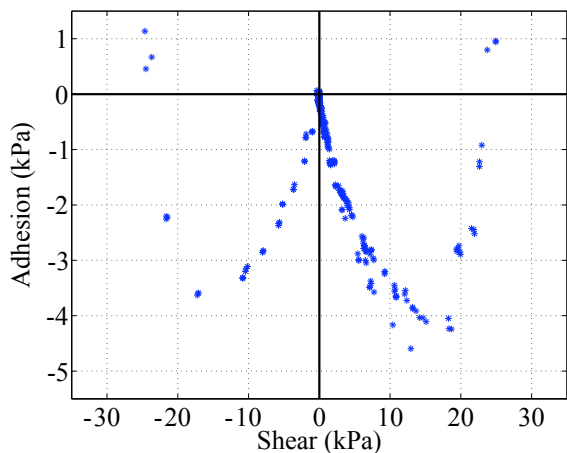


Fig. 4: The limit curve of controllable microwedge adhesive. Positive shear values represent forces applied by the climber down the wall. Negative normal values are adhesion forces applied by the climber into the wall. Note the symmetry of the limit in positive and negative shear. Such symmetry means that the adhesive cannot slide up the wall, unless a method is used to create anisotropic adhesion. Also note that when the shear load is removed, the normal load capacity drops to nearly zero. This effect means that the adhesive can be removed from the wall with nearly no normal force.

where A_{np} is the shear adhesion in the non-preferred direction and A_p in the preferred direction. The hoisting ability, H , can be defined as

$$H = \frac{P_{max}}{BW}, \quad (2)$$

where P_{max} is the maximum payload and BW is the bodyweight. Because adhesion in the non-preferred direction counters the ability of the robot to hoist a load, it follows that

$$A_p - A_{np} = P_{max}. \quad (3)$$

Then the hoisting ability of the robot, H , and consequently the Factor of Safety ($F.S.$) without a load, can be written as

$$H = F.S. = (1 - \alpha) \frac{A_p}{BW}. \quad (4)$$

Without anisotropic adhesion ($\alpha = 1$), a robot using a 1 DOF linear inchworm gait could not climb, nor carry a load. Decreasing α linearly increases the hoisting capability, H . We present two methods for achieving relatively high values of α , one mechanical (for the 9 g robot) and one at the adhesive level (for the 20 mg climber).

For the 9 g climber, the scale is large enough to use a mechanical solution in order to decrease adhesion while the pad moves up the wall. The bottom of the unloaded adhesive pad is brought away from the wall as a result of carefully selected tendon attachment points (Fig. 5, bottom, left). The upper tendon is attached to the pad further from the climbing surface than the lower tendon. When the tension is equal in both tendons, the two tendons align, rotating the pad away from the wall. In contrast, when the tension in the lower

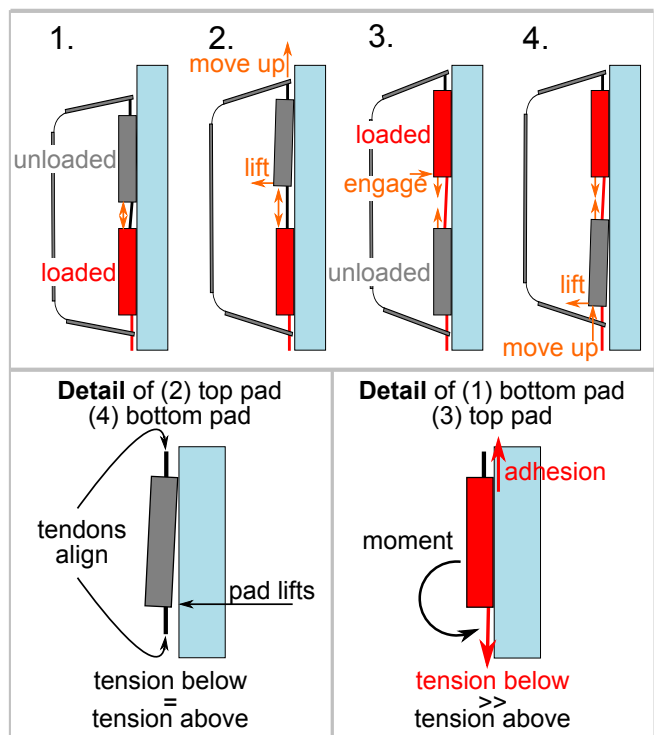


Fig. 5: *Top*, Drawing of the inchworm dry adhesive climbing gait for the 9 g robot. 1) The bottom pad bears the load. 2) The top pad rotates away from the wall when unloaded, and translates upwards (see left detail). 3) The top pad reaches the extent of its travel and begins to take load, coming into contact (see right detail). 4) The top pad takes the entirety of the load, and the lower pad rotates away from the wall and translates upward. *Bottom, left*, Detail of pad lifting. The offset of the attachment points of the tendons (top tendon further from wall) forces a pad to rotate away from the wall when tension is equal in both tendons. *Bottom, right*, Detail of pad engaging. In contrast, when the tension in the top tendon is much less than that in the bottom tendon, the pad rotates into the wall, due to the moment generated by the shear adhesion at the surface and the bottom tendon.

tendon is much greater than that in the upper tendon, the pad begins to move down the wall, the adhesive at the top of the pad engages, and a moment results. This moment is due to the upward shear adhesion acting on the pad at the surface while the downward tendon tension acts at a distance from the surface.

While such a design works at the centimeter scale, it is very difficult at the scale of the 20 mg climber. Therefore we adapted this concept (greatly decreasing the area of adhesive in contact with the surface when the pad is pulled in the non-preferred direction) to be compatible with a sub-centimeter pad. The method involves siping, or making small, angled cuts in the adhesive (Fig. 6). The cuts in the PDMS behind the microwedges do not alter performance when loaded in the preferred direction, but allow for a greatly reduced shear adhesion in the non-preferred direction (See Sec. IV-A). While such one-way adhesion has been

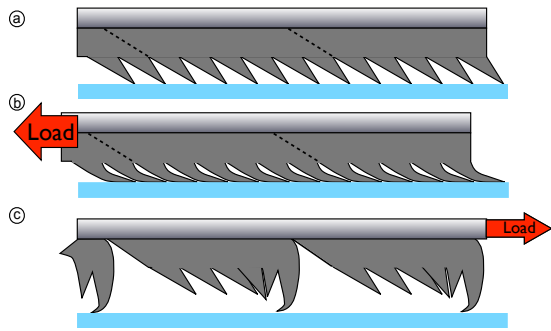


Fig. 6: A) In order to allow the adhesive to move up the wall for the 20 mg robot, a new method of creating a one-way adhesive was developed using siping (dotted lines). B) The cuts remain closed during preferred direction loading, leaving performance unaffected. C) However, when loaded in the non-preferred direction, the cuts open, lifting the majority of the adhesive off of the surface. This greatly decreases adhesion.

previously reported with stiff angled fibers [19], this method makes one-way adhesion available for softer dry adhesives, and shows smaller values of α .

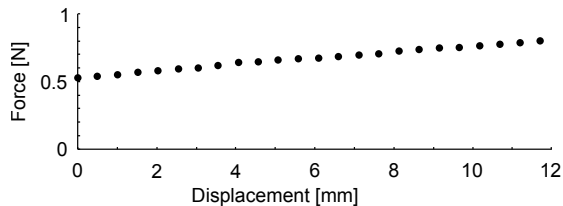


Fig. 7: The force-displacement curve of the return spring. It is desirable to have a nearly constant force that is slightly larger than the small shear force that is required to slide the pad up the wall.

In order to move the upper pad up the wall while unloaded, a return spring is required. Ideally it would be a constant force spring, applying just enough force to slide the pad up the wall. Any additional force in the spring would need to be overcome by the actuator while bringing the pads together. The force-displacement curve of the designed preloaded bow spring shows the desired small change in force across the 10 mm of travel in the spring (Fig. 7).

These three design choices, namely a rigid adhesive pad loaded by a tendon, a controllable adhesive, and an inchworm gait that exploits anisotropic adhesion, allow the creation of very simple, light climbers with large hoisting abilities.

III. DESIGN SPECIFICATIONS AND FABRICATION

With the principles of the designs in place, it is possible to present the details of the two robots, first the 9 g miniature robot, and second the 20 mg micro robot.

A. 9 g Climbing Robot

The 9 g climber is shown in Fig. 8. The main components are the adhesive pads, the servo, the circuit board, the battery,

the tendon, and the return spring (See Tab. I). The dimensions are 30 mm long, 25 mm wide, and 20 mm tall. The adhesive pads are laser machined from fiberglass sheet and directly cast with $80 \mu\text{m}$ tall microwedges on the contacting face. The servo is attached to the top pad with cyanoacrylate adhesive. The circuit board is mounted to the servo with double-sided foam tape, while the battery is attached directly to the top pad, next to the servo. The top tendon is attached to the adhesive pad via a machined hole in the top of the pad and to the return spring via a hole in its end. The return spring is made from 0.7 mm thick Delran, machined by laser, with a section of carbon-fiber bonded to the central portion to give it a squared off shape. The middle tendon is mounted to the a servo horn that is machined into a spool shape. It then passes through a machined hole in the bottom of top pad into a machined hole in the top of the lower pad, where it is fixed. The bottom tendon passes from a machined hole in the bottom pad to the load.

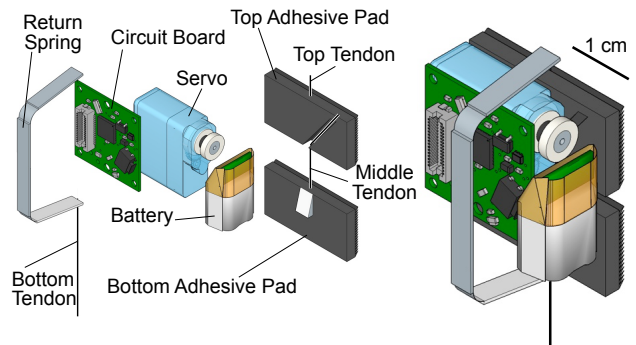


Fig. 8: Drawing of the 9 g climber.

Adhesive Pads (3g)	Material	Fiberglass, PDMS adhesive
	Size (L x W x H)	10 mm x 25 mm x 3 mm
	Max Load	12 N
	Adhesive Cycle Speed	~15Hz
Servo/ Winch (3 g)	Name	Hitec HS-5035HD
	Max Load / Cycle Work	35 N / 0.25 J/stroke
	Max Cycle Rate	~1.5 Hz
	Operating Efficiency	~ 20% under half load
Processor (1 g)	ATMega 328P	8 MHz ("TinyLily")
	Inputs/Outputs	8
Battery (1 g)	Type	Lithium-Polymer
	Capacity	500 J (3.7 V, .040 Amp hr.)
Spring (1 g)	Material	Delrin (0.7 mm thick) with Brass
	Nominal Spring Force	~0.6 N
Tendon	Material	Spectra (0.28 mm Braided)
	Max Load	140 N
Assembled Robot (9 g)	Mass	9g
	Size (L x W x H)	30 mm x 25 mm x 20mm
	Step Size / Step Rate	12 mm / 1.5 Hz (Servo Limited)
	Speed	0.6 body-lengths/s / 1.8cm/s
	Max Payload : Weight	> 100:1
	Max Climbing Height	4 m (theoretical, 1 kg payload)

TABLE I: Specs for the 9 g climber.

B. 20 mg Climber

The micro climber is detailed in Fig. 9. This climber is mostly a proof of concept to show that the gait can be scaled to much smaller robots (this climber is nearly 3 orders of magnitude less massive than the servo driven robot). It comprises two adhesive pads, a coiled spring Shape Memory Alloy (SMA) actuator, tendons, and a return spring (See Tab. II). The adhesive pads are again constructed from fiberglass with microwedge adhesive. Small holes are machined in the top and bottom of each pad, into which Spectra strands (tendons) are passed and fixed with cyanoacrylate. The return spring is made from two pieces of 0.4 mm thick, 1.5 cm long, 2 mm tall fiberglass rectangles attached at the ends with a kevlar flexure. The top tendon passes from the kevlar joint in the return spring the top pad. Another tendon passes from the top pad to the coiled SMA, and a third tendon connects the SMA to the bottom pad. The bottom tendon connects the bottom pad to the bottom of the return spring. Loads are applied through the bottom tendon. The climber does not have onboard power, but instead is activated by a nearby resistive heat source.

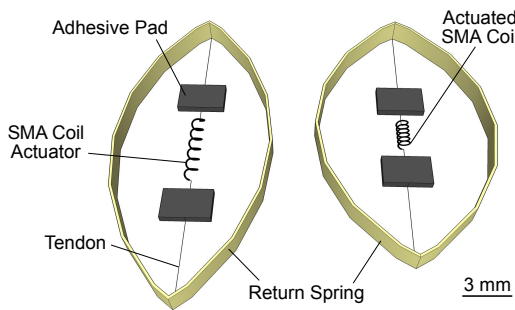


Fig. 9: Drawing of the 20 mg climber.

Adhesive Pads	Material	Fiberglass, PDMS adhesive
	Size (L x W x H)	3 mm x 2 mm x 0.7 mm
	Max Load	0.07 N
	Max Cycle Rate	~15Hz
Actuator	Type	Shape Memory Alloy
	Wire diameter	0.1 mm
	Coil Diameter	0.4 mm
	Max Force	0.15 N
	Max Stroke	1.5 mm
	Max Cycle Rate	~1 Hz (no active cooling)
Power Source	Type	Heat (external)
Spring	Material	Fiberglass (0.4 mm), Kevlar
	Spring Force	.04 N
Tendon	Material	Spectra (0.02 mm filament)
Assembled Robot	Size (L x W x H)	12 mm x 9 mm x 1.5 mm
	Mass	20 mg
	Step Size	0.8 mm
	Step Rate	1 Hz (Actuator Limited)

TABLE II: Specs for the 20 mg climber.

IV. RESULTS

A series of tests were done to help characterize the gait and the climbers.

A. Controllable and Anisotropic Adhesion

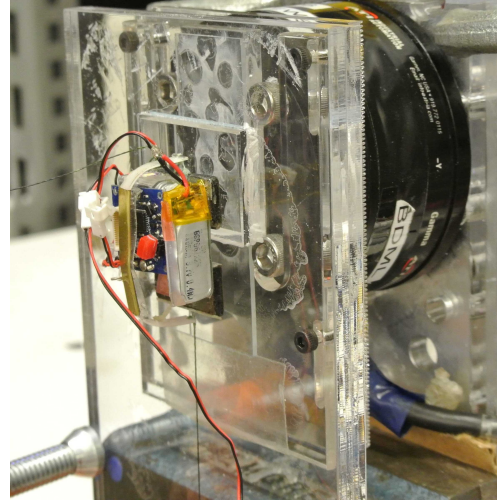


Fig. 10: The experimental setup for measuring the forces during a step of the 9 g climber.

To test the anisotropy ratio, α of the 9 g climber, the robot with a 1 kg payload, was made to step onto a sensorized section of a vertical wall (Fig. 10). The section was supported by an ATI-Gamma 6-axis force-torque sensor reordering at 500 Hz. The results of the test are shown in Fig. 11. In the perpendicular direction, approximately 1 N of force can be seen as the pad moves up along the sensor (A_{np} value). According to Eq. 1, A_{np} divided by the shear adhesion ability of a pad ($A_p = 21$ N) determines the α value: 0.083 (Tab. III). Such a low α value helps create a large hoisting ability, H , according to Eq. 4.

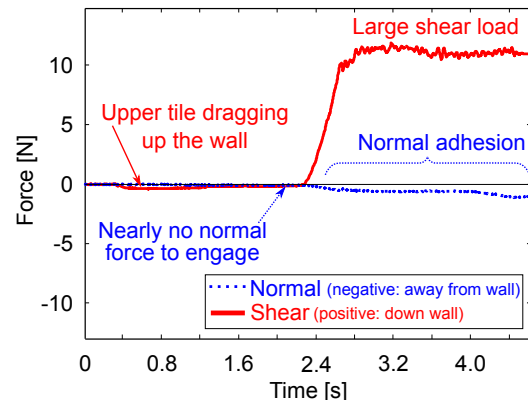


Fig. 11: Force data from a step of the 9 g climber on a vertical surface.

Anisotropy was also tested on for the siping method. Because it was unfeasible to test the 20 mg climber, a 2.5 x 2.5 cm adhesive pad was tested. The pad was placed on a flat glass surface and loaded through a tendon with

Adhesive Type	Shear Stress	Peak Non-Preferred Shear Stress	Anisotropy Ratio, α	Hoisting Ability, H (body weights)	Effective Adhesive Loss
Flat, Smooth PDMS	High	High (Isotropic)	1	0	100%
Standard Controllable Adhesive	70 kPa	51 kPa	0.73	58	73%
Controllable Adhesive Mechanical A.A.	70 kPa	N/A (5.8 kPa effective)	0.083	196	8%
Controllable Adhesive Material A.A.	70 kPa	1.1 kPa	0.016	211	2%
Controllable Adhesive Perfect A.A.	70 kPa	0 kPa	0	223	0%

TABLE III: Anisotropic adhesion data for various adhesives and configurations. Mechanical A.A. (Anisotropic Adhesion) refers to the method used by the 9 g climber. Material A.A. refers to the siping method used in the 20 mg climber.

an Aurora Muscle Lever 309C, which recorded force and displacement data. Results are shown in Fig. 12. While siping does not significantly effect the ability of the adhesive in the preferred direction (statistical P -value = 0.9), in the non-preferred direction, a substantial difference is observed. This is important not only in creating an α value of 0.016, but also for reducing wasted work during climbing. The area under the curves on the the force-displacement plot represent work done by the robot while lifting a pad up the wall. The steady state non-preferred shear adhesion is less than 0.15 N, approximately 200 times less than the adhesive ability in the preferred direction (31 N).

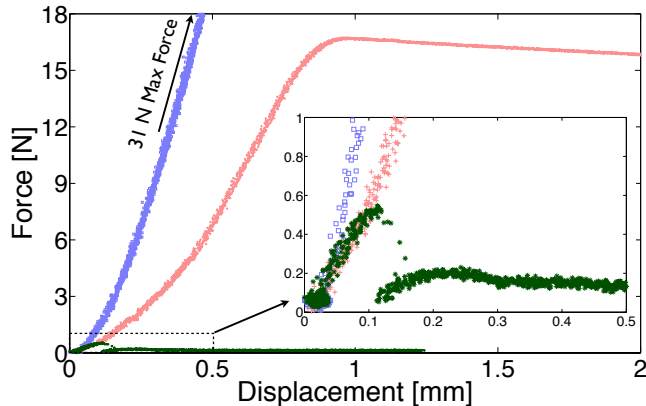


Fig. 12: Force and displacement data from anisotropic adhesion testing. Blue squares show a siped pad loaded in the preferred direction. Red crosses show a non-siped pad loaded in the non-preferred direction. Green stars show a siped pad in the non-preferred direction. Siping greatly reduces the shear adhesion in the non-preferred direction.

B. Speed and Load

The two potential limiters for the speed of the 9 g robot are the adhesives and the servo. Fibrillar adhesives, however, are relatively fast. Unlike a dry adhesive without features,

for which the contact patch must spread across the adhesive area in a progressing line, fibrillar adhesives can break this single serial event into tens of thousands of parallel events. Therefore, the speed to both engage and disengage the fibrillar adhesive can be orders of magnitude faster. Experiments with flat PDMS peeled at 40 degrees from the glass surface have shown that with a peel force of 0.05 N (half the robot's weight), peeling occurs at 1 mm/s [20]. For flat PDMS, this would take 12 s to make it across a pad, but only 0.08 s to make it across all of the 90 μm contact patches of the microwedges in parallel (which each peels like a flat PDMS film). Since engagement happens at a similar rate, the predicted maximum frequency f_{max} of the robot is

$$f_{max} = \frac{1}{2(t_{eng} + t_{dis})} \quad (5)$$

where t_{eng} is the time to fully engage and t_{dis} is the time to disengage. The factor of two results from the need to have both adhesive pads engage and disengage during each cycle. With t_{dis} roughly 0.08 s, and with the assumption that t_{eng} is roughly equivalent, f_{max} is predicted to be less than 15 Hz.

However, the limit of 50 Hz is never reached, because of the limit of the servo. The no load speed is 540°/s, and since the servo turns forward and back 180° per step, the max speed without load is 1.5 Hz. Experiments to measure speed and step size found roughly a 12 mm step and a speed of 18 mm/s, or 0.6 bodylengths/s. At full load of 1000 g, the robot was measured to climb at 3-4 mm/s, although the gait was not optimized for speed.

C. Robustness to Missed Steps

The 9 g climber shows very desirable characteristic in its robustness to a missed step (where the adhesive does not engage with the surface). In most climbing robots, a missed step is catastrophic, because the outgoing pad is peeled from the wall in order to press the incoming pad into contact. This means that if the incoming foot does not engage, the robot has no feet left in contact (in the case of a gait where only half of the feet are on the wall during stance—some climbing robots climbed with 6 feet and only removed one at a time [21]). In contrast, the presented inchworm climbing gait is only able to release the outgoing foot by applying a shear force from the incoming foot. Therefore, if the incoming foot does not engage, the outgoing foot remains firmly planted, until a second step is attempted. Frames from a video in which the incoming foot is set up to fail on the first attempt shows the described robustness (Fig. 13).

D. Payload to Required Power Ratio

The 9 g climber displays a large ratio of load carrying ability to required power for climbing. Fig. 14, blue dots, shows the power consumed by the 9 g climber while hoisting loads from 300 to 1100 g. At a 1000 g payload, this ratio is roughly 2 kg/W. For reference, Stickybot III could manage 0.2 kg/W. As another comparison, the available power from an off-the-shelf solar system (Nomad 7 Solar Panel, Goal

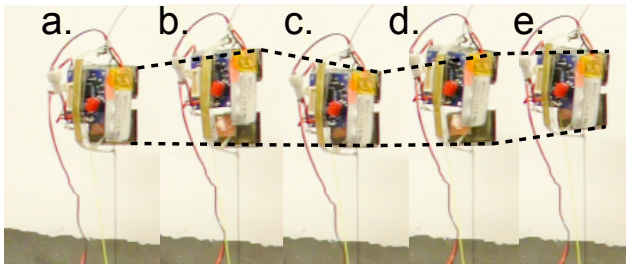


Fig. 13: Frames from a video of the 9 g climber showing robustness to missed steps. The top foot is made to not engage in (b-c), but the robot does not fall (d), but rather attempts a second time and succeeds (e).

Zero, Inc.) is plotted (red diamonds). If the entire payload were panels, 14 W more power would be supplied than required for climbing. Alternatively, only roughly 50 g (5% of the load capacity) of solar panel is needed to carry a 1100 g payload. This leaves both the power and the payload capability to carry significant tools and communication devices.

As another point of reference, if the entire payload were composed of non-rechargeable lithium batteries, the robot could theoretically climb 10 km vertically. Obviously, the robot would not survive this number of steps, however, it is an informative metric for understanding the scale of the payload to power required ratio.

The robot also demonstrates an ability to park while drawing no power from the actuator (Fig. 14, green squares). This capability is created through bypassing the actuator when transferring load to the bottom adhesive pad. The circuit board draws 0.04 W, but this can be set to sleep mode, decreasing the draw to 4 mW. Such an ability is beneficial for any environmental monitoring tasks that may require extended periods of time in a parked state.

V. CONCLUSIONS AND FUTURE WORK

In this work, we presented the design principles that allowed the creation of small, simple climbers capable of hoisting payloads equivalent to many times the weight of the climbers. The proposed design principles describe a novel inchworm climbing gait that leverages controllable and anisotropic dry adhesion. The designs of both a 9 g and 20 mg climber were presented. Data from testing the anisotropic adhesion showed up to a factor of 200 difference in preferred and non-preferred direction shear adhesion. Results from testing the larger climber showed speeds of up to 0.6 bodylengths/s at light loads and payloads of up to 1100 g. The robot also demonstrated a robustness to missed steps, a large ratio of hoisting ability to required power, and a nearly power-free parking stance. The 20 mg climber took steps at 0.2 Hz and could carry 500 mg.

The results from the 9 g climber show that attaining the level of hoisting ability of a weaver ant is possible in a small robotic climbing platform using controllable, anisotropic adhesion. Additionally, the 20 mg climber, while inefficient and slow, shows that climbing with dry adhesive and hoisting

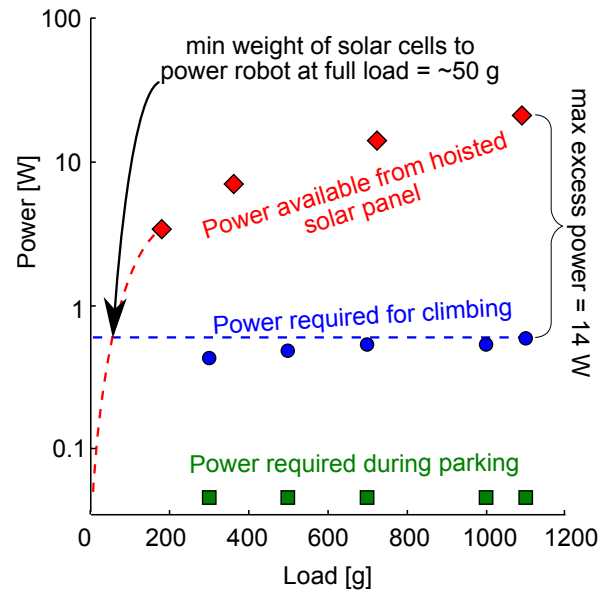


Fig. 14: In blue circles, data showing the power required for the 9 g robot to carry various loads. In red diamonds is the power delivered by commercially available solar units (Nomad 7). If the power per weight roughly scales linearly, only 50 g of solar cells is required to climb continuously with a 1000 g payload. Hoisting a full payload of solar cells would provide 14 W of power beyond what the robot requires for climbing.

is possible at a much smaller scale than has ever been demonstrated. While the climbers do not show functionality beyond vertical climbing, we hope that the concepts presented in this paper will aid in the development of small, highly functional, mobile robots capable of applying large forces to their environments. With such a large margin for payload, the climbers have plenty of capacity for added functionality.

Future work for these two robots presents many opportunities. First, adding further functionality to the 9 g climber, including robust turning and climbing downwards, is a first priority. Initial investigations in the realm show promise: two SMA actuators can pull the top pad to one side or the other for turning, and adding a simple mechanical switch actuated with SMA allows downward climbing. Adding material level anisotropy to the 9 g climber could further increase its efficiency. For the 20 mg climber, two parallel SMA actuators could allow turning. Creating an external heat source that could work over a long range, such as a laser, could power a large number of 20 mg climbers on a wall from a distance. Adding sensing is also desirable, such as line following for climbing up buildings. Another goal is to add the ability to step over obstacle, like a real inchworm does. This may involve a second small actuator or a linkage. The ability to climb rough, exterior surfaces could be added by integrating microspines [22] with the dry adhesive. With recent work on physical swarms of robots progressing rapidly [23], creating a large group of climbing robots with the ability to move tens of kilograms up a vertical surface is an intriguing future direction.

ACKNOWLEDGMENTS

Elliot Hawkes was supported by the NSF Graduate Research Fellowship. David Christensen was supported by SRI and DARPA HR0011-12-C-0040.

REFERENCES

- [1] W. Federle, W. Baumgartner, and B. Hölldobler, "Biomechanics of ant adhesive pads: frictional forces are rate-and temperature-dependent," *Journal of Experimental Biology*, vol. 207, no. 1, pp. 67–74, 2004.
- [2] J. Wojtusiak, E. Godzińska, and A. Dejean, "Capture and retrieval of very large prey by workers of the african weaver ant, *oecophylla longinoda* (latreille 1802)," *Tropical Zoology*, vol. 8, no. 2, pp. 309–318, 1995.
- [3] W. Federle and T. Endlein, "Locomotion and adhesion: dynamic control of adhesive surface contact in ants," *Arthropod structure & development*, vol. 33, no. 1, pp. 67–75, 2004.
- [4] S. Kim, M. Spenko, S. Trujillo, B. Heyneman, D. Santos, and M. R. Cutkosky, "Smooth vertical surface climbing with directional adhesion," *Robotics, IEEE Transactions on*, vol. 24, no. 1, pp. 65–74, 2008.
- [5] E. W. Hawkes, J. Ulmen, N. Esparza, and M. R. Cutkosky, "Scaling walls: Applying dry adhesives to the real world," in *Intelligent Robots and Systems (IROS), 2011 IEEE/RSJ International Conference on*. IEEE, 2011, pp. 5100–5106.
- [6] M. P. Murphy, C. Kute, Y. Mengüç, and M. Sitti, "Waalbot ii: adhesion recovery and improved performance of a climbing robot using fibrillar adhesives," *The International Journal of Robotics Research*, vol. 30, no. 1, pp. 118–133, 2011.
- [7] M. Greuter, G. Shah, G. Caprari, F. Tâche, R. Siegwart, and M. Sitti, "Toward micro wall-climbing robots using biomimetic fibrillar adhesives," in *Proceedings of the 3rd International Symposium on Autonomous Minirobots for Research and Edutainment (AMiRE 2005)*. Springer, 2006, pp. 39–46.
- [8] E. W. Hawkes, E. V. Eason, D. L. Christensen, and M. R. Cutkosky, "Human climbing with efficiently scaled gecko-inspired dry adhesives," *Journal of the Royal Society Interface*, in press.
- [9] K. Autumn, "Properties, principles, and parameters of the gecko adhesive system," in *Biological adhesives*. Springer, 2006, pp. 225–256.
- [10] K. Kotay and D. Rus, "The inchworm robot: A multi-functional system," *Autonomous Robots*, vol. 8, no. 1, pp. 53–69, 2000.
- [11] P. Dario, P. Ciarletta, A. Menciassi, and B. Kim, "Modeling and experimental validation of the locomotion of endoscopic robots in the colon," *The International Journal of Robotics Research*, vol. 23, no. 4-5, pp. 549–556, 2004.
- [12] J. Lim, H. Park, J. An, Y.-S. Hong, B. Kim, and B.-J. Yi, "One pneumatic line based inchworm-like micro robot for half-inch pipe inspection," *Mechatronics*, vol. 18, no. 7, pp. 315–322, 2008.
- [13] Y. Guan, H. Zhu, W. Wu, X. Zhou, L. Jiang, C. Cai, L. Zhang, and H. Zhang, "A modular biped wall-climbing robot with high mobility and manipulating function," *Mechatronics, IEEE/ASME Transactions on*, vol. 18, no. 6, pp. 1787–1798, 2013.
- [14] D. Lee, S. Kim, Y.-L. Park, and R. J. Wood, "Design of centimeter-scale inchworm robots with bidirectional claws," in *Robotics and Automation (ICRA), 2011 IEEE International Conference on*. IEEE, 2011, pp. 3197–3204.
- [15] J.-S. Koh and K.-J. Cho, "Omega-shaped inchworm-inspired crawling robot with large-index-and-pitch (lip) sma spring actuators," *Mechatronics, IEEE/ASME Transactions on*, vol. 18, no. 2, pp. 419–429, 2013.
- [16] S. Hollar, A. Flynn, C. Bellew, and K. Pister, "Solar powered 10 mg silicon robot," in *Micro Electro Mechanical Systems, 2003. MEMS-03 Kyoto. IEEE The Sixteenth Annual International Conference on*. IEEE, 2003, pp. 706–711.
- [17] Y. Liu, C. Hu, X. Wu, Y. Zhang, T. Mei, and S. Sun, "Design of vertical climbing robot with compliant foot," in *Robotics and Biomimetics (ROBIO), 2012 IEEE International Conference on*. IEEE, 2012, pp. 649–654.
- [18] P. Day, E. V. Eason, N. Esparza, D. Christensen, and M. Cutkosky, "Microwedge machining for the manufacture of directional dry adhesives," *Journal of Micro and Nano-Manufacturing*, vol. 1, no. 1, p. 011001, 2013.
- [19] J. Lee, R. S. Fearing, and K. Komvopoulos, "Directional adhesion of gecko-inspired angled microfiber arrays," *Applied Physics Letters*, vol. 93, no. 19, p. 191910, 2008.
- [20] B.-m. Z. Newby and M. K. Chaudhury, "Friction in adhesion," *Langmuir*, vol. 14, pp. 4865–4872, 1998.
- [21] M. Spenko, G. C. Haynes, J. Saunders, M. R. Cutkosky, A. A. Rizzi, R. J. Full, and D. E. Koditschek, "Biologically inspired climbing with a hexapedal robot," *Journal of Field Robotics*, vol. 25, no. 4-5, pp. 223–242, 2008.
- [22] A. T. Asbeck, S. Kim, M. R. Cutkosky, W. R. Provancher, and M. Lanzetta, "Scaling hard vertical surfaces with compliant microspine arrays," *The International Journal of Robotics Research*, vol. 25, no. 12, pp. 1165–1179, 2006.
- [23] M. Rubenstein, A. Cornejo, and R. Nagpal, "Programmable self-assembly in a thousand-robot swarm," *Science*, vol. 345, no. 6198, pp. 795–799, 2014.